ICJK
Chinese Journal of Information Fusion
http://dx.doi.org/10.62762/CJIF.2024.841250

RESEARCH ARTICLE

Basic Belief Assignment Determination Based on Radial Basis Function Network

Wei Li[1], **Deqiang Han**[1,*], **Jean Dezert**[2] **and Yi Yang**[3]

[1] School of Automation Science and Engineering, Xi'an Jiaotong University, Xi'an 710049, China
[2] The French Aerospace Lab, Chemin de la Hunière, F-91761 Palaiseau, France
[3] School of Aerospace, Xi'an Jiaotong University, Xi'an 710049, China

Abstract

In Dempster-Shafer evidence theory (DST), the determination of basic belief assignment (BBA) is an important yet challenging issue before the evidence fusion. The rational mass determination of compound focal elements is crucial for fully taking advantage of DST, i.e., the ability to represent the ambiguity. In this paper, for the compound focal elements, we select and construct the "compound-class samples" with ambiguous class membership. Then, we use these samples to construct an end-to-end model called Evidential Radial Basis Function Network (E-RBFN), with the input as the sample and the output as the corresponding BBA. The E-RBFN can directly determine the mass values for all focal elements (including the singleton and compound ones).Experimental results of evidence decision-based pattern classification on multiple UCI and image datasets show that our proposed method is rational and effective.

Academic Editor:
Jun Liu

Submitted: 25 August 2024
Accepted: 22 October 2024
Published: 07 December 2024

Vol. 1, **No.** 3, 2024.
10.62762/CJIF.2024.841250

***Corresponding author:**
✉ Deqiang Han
deqhan@xjtu.edu.cn

Keywords: Dempster-Shafer evidence theory, evidence fusion, basic belief assignment, uncertainty modeling, radial basis function network, pattern classification.

1 Introduction

Dempster-Shafer evidence theory (DST) [1, 2], also known as the theory of belief functions, is an important mathematical framework for uncertainty modeling and reasoning. It has been widely applied in several fields, such as information fusion [3, 4], pattern classification [5, 6], and multi-attribute decision-making [7, 8].

In DST, the determination (or generation) of BBA corresponds to the modeling of uncertainty [9], which currently remains a challenging issue. The methods for determining BBA are often related to the specific applications. For automatic target classification, Selzer *et al.* [10] proposed a BBA determination method using the class number and the target's neighborhood. Bi *et al.* [11] proposed a focal element triplet-based method for text classification. Zhang *et al.* [12] proposed to determine BBA using the evidential Markov random field for the image segmentation problem. For image edge detection, Dezert *et al.* [13] determined BBA to describe the uncertainty of the chosen threshold. For multi-attribute decision-making, Han *et al.* [7]

Citation
Li, W., Han, D., Dezert, J., & Yang, Y. (2024). Basic Belief Assignment Determination Based on Radial Basis Function Network. *Chinese Journal of Information Fusion*, 1(3), 175–182.

determined BBA using the intervals of the expected payoffs for different alternatives.

In addition, some general BBA determination methods have been proposed. Jiang *et al.* [14] proposed a BBA determination method based on the triangular fuzzy number. Han *et al.* [15] proposed a method for transforming the fuzzy membership function into BBA using uncertain optimization. Kang *et al.* [16] proposed an interval number-based BBA determination method.

For BBA determination, the rational mass determination of compound focal elements is crucial for fully taking advantage of DST (i.e., the capability to represent and handle the ambiguity). However, when determining the mass value of compound focal elements, traditional methods are often heuristic and lack sufficient soundness, such as the method using singleton focal elements' complement set [11] or the method using discount to singleton focal elements[17]. In this paper, for the compound focal elements, we first select and construct "compound-class samples", defined as samples with ambiguous class membership. Based on these samples, we construct an end-to-end model called Evidential Radial Basis Function Network (E-RBFN), where the input is the sample and the output is the corresponding BBA. That is, the E-RBFN can directly determine the mass values for all focal elements (including the singleton and compound ones). Experimental results of evidence fusion decision-based pattern classification on multiple UCI and image datasets show that our proposed method performs better than many existing BBA determination methods.

2 Preliminary

2.1 Basics of Dempster Shafer Theory

In DST, the frame of discernment (FOD) is defined as a set consisting of n mutually exclusive and exhaustive elements, denoted by $\Theta = \{\theta_1, \theta_2, \ldots, \theta_n\}$. Let 2^Θ be the power set of the FOD Θ. If a set function $m : 2^\Theta \to [0, 1]$ satisfies

$$\sum_{A\subseteq\Theta} m(A) = 1, m(\emptyset) = 0 \tag{1}$$

then m is called a basic belief assignment (BBA, also called a mass function). A is called a focal element of the BBA $m(\cdot)$ if and only if $m(A) > 0$.

Given a BBA on the FOD Θ, the belief function Bel and plausibility function Pl are respectively defined as

$$Bel(A) = \sum_{B\subseteq A} m(B), \forall A \subseteq \Theta \tag{2}$$

$$Pl(A) = \sum_{B\cap A\neq\emptyset} m(B), \forall A \subseteq \Theta \tag{3}$$

The $Bel(A)$ and $Pl(A)$ constitute the lower and upper bounds of the belief interval $[Bel(A), Pl(A)]$, which represents the degree of imprecision for the proposition A.

Suppose that m_1 and m_2 are two independent BBAs on the same FOD, which can be combined via the Dempster's rule of combination [1] as follows

$$m(A) = \begin{cases} 0, A = \emptyset \\ \frac{\sum_{B\cap C=A} m_1(B)m_2(C)}{1-K}, A \neq \emptyset \end{cases} \tag{4}$$

where $K = \sum_{B\bigcap C=\varnothing} m_1(B)m_2(C)$ is the conflict coefficient between the two BBAs.

The pignistic probability [18] corresponding to a BBA m is defined as

$$BetP(\theta_i) = \sum_{\theta_i\in B} \frac{m(B)}{|B|}, \forall B \subseteq \Theta \tag{5}$$

where $|B|$ is the cardinality of the focal element B. Based on this, one can perform probabilistic decisions according to the decision rule defined as follows.

$$i^* = \arg\max_i BetP(\theta_i) \tag{6}$$

2.2 Traditional BBA Determination Methods

1) BBA Determination Using Discount to Singletons [17]: Suppose that FOD $\Theta = \{\theta_1.\theta_2, \ldots, \theta_n\}$, given an input sample x, the probability for each class is first obtained by a well-trained classifier (such as the fully-connected neural network), represented as $p_1(x), p_2(x), \ldots, p_n(x)$. Then, the mass value for each singleton focal element is calculated by applying a discount to the corresponding probability, as shown in Eq. (7).

$$m(\{\theta_i\}) = \alpha p_i(x) \tag{7}$$

where α is the discount factor designed by users, with values ranging from $[0, 1]$. Finally, the mass value for the compound focal element Θ is calculated by Eq. (8).

$$m(\Theta) = 1 - \alpha \sum_{i=1}^{n} p_i(x) \tag{8}$$

For example, if the FOD $\Theta = \{\theta_1, \theta_2, \theta_3\}$, given a test sample, its probabilities corresponding to each class are first obtained using a trained classifier (a fully-connected neural network), represented as $p_1(x) = 0.56, p_2(x) = 0.12, p_3(x) = 0.32$.

If the discount factor is set to 0.8, the corresponding BBA for this sample is represented as $m(\{\theta_1\}) = 0.8 \times 0.56 = 0.448, m(\{\theta_2\}) = 0.8 \times 0.12 = 0.096, m(\{\theta_3\}) = 0.8 \times 0.32 = 0.256, m(\Theta) = 1 - \sum_{i=1}^{3} m(\{\theta_i\}) = 0.2$.

2) BBA Determination Using Tri-Focal Element [11]: Suppose that FOD $\Theta = \{\theta_1, \theta_2, \ldots, \theta_n\}$, given an input sample x, the probability for each class is first obtained by a well-trained classifier (such as the fully-connected neural network), represented as $p_1(x), p_2(x), \ldots, p_n(x)$. Define the tri-focal element as $\langle A_1, A_2, A_3 \rangle$, where A_1, A_2 are singleton focal elements, and A_3 is compound focal element, defined as

$$\begin{cases} A_1 = \{\theta_{i_1}\}, & i_1 = \arg\max\limits_{j} p_j \\ A_2 = \{\theta_{i_2}\}, & i_2 = \arg\max\limits_{j, j \neq i_1} p_j \\ A_3 = \Theta \end{cases} \tag{9}$$

The mass values of A_1, A_2 and A_3 are respectively calculated by Eq.(10).

$$\begin{cases} m(A_1) = p_1(x), \\ m(A_2) = p_2(x), \\ m(A_3) = 1 - m(A_1) - m(A_2) \end{cases} \tag{10}$$

For example, if the FOD $\Theta = \{\theta_1, \theta_2, \theta_3\}$, given a test sample, its probabilities corresponding to each class are first obtained $p_1(x) = 0.12, p_2(x) = 0.38, p_3(x) = 0.50$. For the tri-focal element $\langle A_1, A_2, A_3 \rangle$, A_1 is defined as $\{\theta_3\}$. A_2 is defined as $\{\theta_2\}$. A_3 is defined as Θ. Then, the mass value of each focal element is calculated as $m(\{\theta_3\}) = 0.50, m(\{\theta_2\}) = 0.38, m(\Theta) = 1 - 0.50 - 0.38 = 0.12$. For the BBA determination, the rational mass determination for compound focal elements is crucial, which is related to fully taking advantage of DST, i.e., the capability to represent ambiguity. However, in the above methods, the mass values of compound focal elements are heuristically determined using the singleton focal elements' mass values (by the complementary set). These approaches lack sufficient witness. To address this, we propose an end-to-end BBA determination method based on a radial basis function network (RBFN), which can directly determine the mass values for all focal elements (including the singleton and compound ones), detailed in Section 3.

3 BBA Determination Based on E-RBFN

In this paper, we propose to design the BBA determination as an end-to-end model called E-RBFN, with the sample as input and the corresponding BBA as the output. Our proposed method is divided into two parts. First, we select and construct the "compound-class samples" with ambiguous class membership, which corresponds to the compound focal elements in the FOD Θ. Second, we treat the compound classes as new class labels to construct the E-RBFN (together with the crisp classes), thus implementing the mass modeling for all focal elements (including the singleton and compound ones).

3.1 Selection of Compound-Class Samples

Before constructing the E-RBFN, we first select and construct the compound-class samples. In this paper, compound-class samples are defined as samples with ambiguous class membership, which corresponds to compound focal elements in the FOD Θ. For example, if a sample belongs to the compound class $\{\theta_1, \theta_2\}$, it represents that the sample's class membership is ambiguous between the crisp class $\{\theta_1\}$ and crisp class $\{\theta_2\}$. In this paper, we propose to use the confusion matrix and the information entropy to select and construct compound-class samples, as shown in Figure 1.

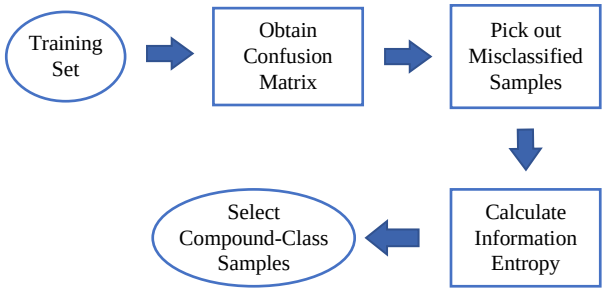

Figure 1. Procedure of compound-class samples selection.

1) Step1-Construct Confusion Matrix: First, we use the cross validation (via the naive Bayesian classifier) to construct confusion matrix. Suppose that FOD $\Theta = \{\theta_1, \theta_2, \theta_3\}$, the confusion matrix is shown in Figure 2.

2) Step2-Pick out Misclassified Samples: Based on the confusion matrix, we pick out the misclassified samples to serve as the compound-class samples. Meanwhile, the correctly classified samples are considered as crisp-class samples.

3) Step3-Calculate Information Entropy: To measure the ambiguity of misclassified samples, we calculate the

		Predicted Label		
		Class 1	Class 2	Class 3
Actual Label	Class 1	$\{\theta_1\}$	$\{\theta_1,\theta_2\}$	$\{\theta_1,\theta_3\}$
	Class 2	$\{\theta_1,\theta_2\}$	$\{\theta_2\}$	$\{\theta_2,\theta_3\}$
	Class 3	$\{\theta_1,\theta_3\}$	$\{\theta_2,\theta_3\}$	$\{\theta_3\}$

Figure 2. Construction of confusion matrix.

information entropy of each misclassified sample. For a misclassified sample x, its information entropy is calculated as follows.

$$H(x) = -\sum_{i=1}^{C} p_i(x)\log_2(p_i(x)) \tag{11}$$

where $p_i(x)$ is the probability for the sample x belonging to the crisp class i (obtained by the Bayesian classifier). C is the total number of the crisp classes. Higher entropy indicates that the probabilities of each class are more similar, implying greater ambiguity.

4) *Step4-Select Compound-Class Samples:* After calculating the entropy for each misclassified sample, we compare it with a predefined threshold (we set it to 1 for the simplicity; other values can also be used). For a sample misclassified between class 1 and class 2 (as an example), if its entropy exceeds the threshold, this sample is assigned to the total set $\{\Theta\}$. If its entropy is less than the threshold, this sample is assigned to the compound class $\{\theta_1, \theta_2\}$. The illustrative example of the compound-class samples selection is provided in Section 3.3.

3.2 Construction of E-RBFN

After obtaining the compound-class samples, we treat them as new classes to construct E-RBFN together with crisp-class samples, thus implementing the mass modeling for each focal element (including the compound focal element). For the dataset containing three crisp classes, there are seven class labels: $\{\theta_1\}$, $\{\theta_2\}$, $\{\theta_3\}$, $\{\theta_1, \theta_2\}$, $\{\theta_1, \theta_3\}$, $\{\theta_2, \theta_3\}$ and $\{\theta_1, \theta_2, \theta_3\}$. The structure of E-RBFN is shown in Figure 3. Note that some classes are omitted.

As shown in Figure 3, the input of E-RBFN is the data sample, and the output is the corresponding BBA. This end-to-end modal can directly determine the mass values for all compound focal elements.

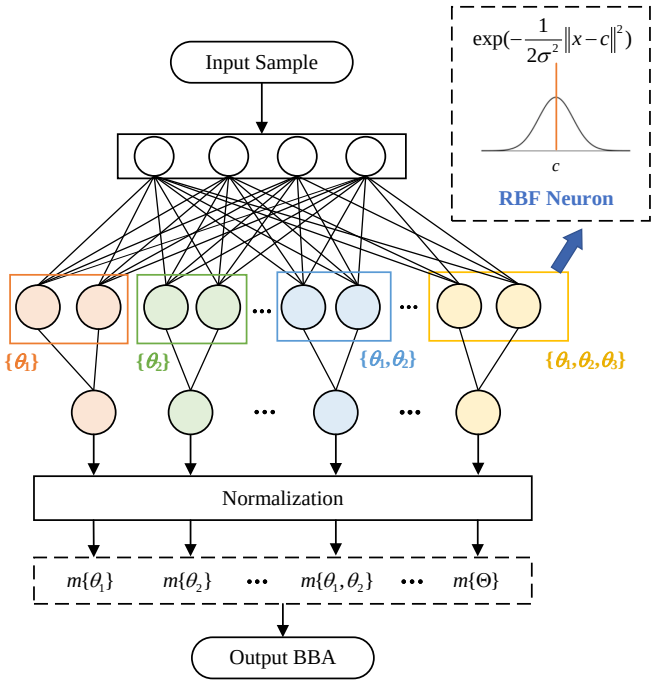

Figure 3. The structure of E-RBFN.

In the structure of E-RBFN, we use the RBF neuron to represent the local region of each class (including the crisp class and the compound class). The activation function of the RBF neuron is defined as the radial basis function, as calculated in Eq. (12).

$$R(x - c_a^n) = \exp(-\frac{1}{2\sigma^2}\|x - c_a^n\|^2) \tag{12}$$

where x is the input sample. c_a^n is the n-th RBF neuron center of class a. σ^2 is the variance of each RBF neuron.

In this paper, the RBF neuron centers are obtained by the k-means clustering algorithm [19]. For example, for the compound class $\{\theta_1, \theta_2\}$, we implement the k-means algorithm in all samples belonging to this class, and then designate the cluster centers as the RBF neuron centers for $\{\theta_1, \theta_2\}$. For the variance of the RBF neuron, we calculate it by the empirical formula [20].

$$\sigma = \frac{d_{\max}}{\sqrt{2h}} \tag{13}$$

where $d_{\max}$ is the maximum distance between the centers of RBF neurons, h is the number of RBF neurons.

3.3 E-RBFN's Application in Pattern Classification

In this section, we use an example to illustrate the process of our E-RBFN-based BBA determination method and its application in pattern classification, with the whole procedure shown in Figure 4. We

use the Iris dataset [21] as an example to show our method. This dataset comprises 150 samples, distributed equally among three classes: Setosa (Se), Versicolor (Ve), and Virginica (Vi). We select 25 samples from each class to serve as the training set.

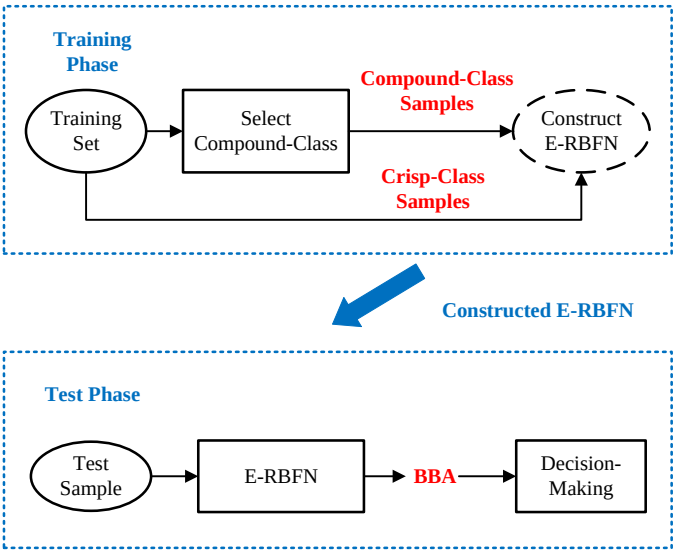

Figure 4. Procedure of E-RBFN-based pattern classification.

1) Select Compound-Class Samples: First, we select the compound-class samples using the confusion matrix and information entropy. Here, the confusion matrix is constructed by the cross validation (with the Bayesian decision) on training datasets, as shown in Table 1.

Table 1. Confusion matrix of Iris dataset.

Size		Predicted Class		
		Se	*Ve*	*Vi*
Actual Class	*Se*	20	3	2
	Ve	4	16	5
	Vi	4	3	18

Then, we pick out the misclassified samples and calculate the corresponding entropy. For a sample misclassified between class Se and Ve, if its entropy exceeds the threshold (set to 1), the misclassified sample is classified as $\{Se, Ve, Vi\}$. If its entropy is less than the threshold, it is classified as $\{Se, Ve\}$.

2) Construct E-RBFN: After selecting compound-class samples, we treat the compound classes as new class labels and construct the E-RBFN together with the crisp-class samples. In this example, there are seven classes: $\{Se\}$, $\{Ve\}$, $\{Vi\}$, $\{Se, Ve\}$, $\{Se, Vi\}$, $\{Ve, Vi\}$ and $\{Se, Ve, Vi\}$. The k-means clustering algorithm is implemented on each class to obtain the RBF neuron centers (k is set to 2). The variance of each RBF neuron is calculated by Eq. (13).

3) BBA Determination Based on E-RBFN: Once the E-RBFN is constructed, it can be used for BBA determination to support the decision-making. To show this process, we select a test sample belonging to the Se class as an example. The feature values of this sample are as $SL = 5.1\ cm$, $SW = 3.5\ cm$, $PL = 1.4\ cm$, $PW = 0.2\ cm$.

The selected sample is the input of the E-RBFN. Then, the E-RBFN can determine the mass values for each focal elements (including the singleton and compound ones) in an end-to-end manner, as $m(\{\theta_1\}) = 0.9032, m(\{\theta_2\}) = 0.0054, m(\{\theta_3\}) = 0.0129$, and $m(\{\theta_1, \theta_2\}) = 0.0171, m(\{\theta_1, \theta_3\}) = 0.0389, m(\{\theta_2, \theta_3\}) = 0.0018, m(\Theta) = 0.0207$.

Next, we transform this BBA into pignistic probability using Eq. (5), and we obtain $BetP(\{Se\}) = 0.9381, BetP(\{\text{Ve}\}) = 0.0218, BetP(\{Vi\}) = 0.0401$. Finally, the test sample is classified as Se, which is consistent with the actual label.

4 Experiments

In the section, we conduct the evidence decision-based pattern classification experiments on multiple UCI [21] datasets and image datasets (from the Kaggle platform [22]) to evaluate the effectiveness of our proposed BBA determination method. The characteristics of these datasets are shown in Table 2.

Table 2. Characteristics of datasets used.

Dataset	Type	Class	Instance
WDBC	UCI	2	569
Thyroid		3	215
CMC		3	1473
Robot		4	5456
Vowel		6	871
Blood Cell	Image	4	12500
Crop Diseases		5	21397
CIFAR-10		10	60000
Fashion-MNIST		10	70000

In the experiments, we compare the classification performance of our method with several traditional BBA determination methods: tri-focal element method [11], discount-based method [17], triangular fuzzy number (TFN)-based method [14] and interval number(IN)-based method [16]. For the E-RBFN, we set the number of layers to 3: the input layer corresponds to the sample feature dimensions, the middle layer is the RBF layer, and the output layer corresponds to the dimensions of the BBA. In the RBF layer, the number of RBF neurons for each class

Table 3. Experimental results of evidence fusion decision-based pattern classification.

	Average ± Std/%	Triplet	Discount	TFN	IN	E-RBFN
WDBC	**Accuracy**	89.72±1.37	88.60±1.45	90.91±1.47	89.16±1.68	**91.46±1.88**
	Precision	89.86±2.45	88.01±1.71	90.72±0.98	88.91±2.06	**91.82±0.86**
	Recall	88.45±1.24	89.16±0.43	**91.10±0.83**	90.21±2.52	90.74±2.13
	F1-Score	88.93±1.82	88.25±1.82	90.91±1.17	90.54±0.64	**91.09±0.81**
Thyroid	**Accuracy**	90.85±1.55	90.06±1.86	93.21±1.74	91.28±0.96	**93.94±2.40**
	Precision	90.28±1.91	90.53±1.50	92.56±1.63	92.14±0.88	**94.15±0.98**
	Recall	91.02±2.41	89.94±1.23	93.34±0.28	91.66±0.51	**94.05±0.85**
	F1-Score	90.57±0.34	90.05±0.51	92.78±0.36	91.89±1.97	**93.98±0.32**
CMC	**Accuracy**	62.12±1.36	62.36±1.32	64.52±0.64	63.29±1.23	**66.94±1.66**
	Precision	62.23±1.91	62.87±0.43	63.94±2.12	62.48±0.85	**65.89±0.97**
	Recall	61.57±1.08	61.89±1.82	64.61±1.52	63.12±0.48	**66.45±2.15**
	F1-Score	61.81±1.91	62.02±0.53	64.00±0.64	62.63±1.94	**66.16±0.88**
Robot	**Accuracy**	92.34±0.69	91.15±1.59	94.48±0.47	93.72±1.36	**95.41±1.23**
	Precision	92.76±1.36	91.89±1.32	94.43±0.64	93.58±1.23	**95.69±1.15**
	Recall	93.12±1.59	92.55±1.64	**95.28±1.15**	94.24±0.64	95.12±2.37
	F1-Score	92.81±2.48	92.04±0.95	94.79±1.88	93.68±1.52	**95.26±0.35**
Vowel	**Accuracy**	91.24±1.36	92.05±1.31	93.19±2.17	94.32±2.00	**95.42±1.02**
	Precision	91.67±1.88	91.02±2.41	92.74±1.79	94.67±1.94	**95.19±1.76**
	Recall	92.14±2.07	91.56±1.18	93.25±0.95	93.45±1.25	**96.03±0.88**
	F1-Score	91.52±1.27	91.18±0.91	92.84±1.54	94.01±2.37	**95.29±0.69**
Blood Cell	**Accuracy**	94.12±1.08	94.15±2.28	95.55±1.39	95.92±1.64	**96.57±1.63**
	Precision	94.24±1.39	93.89±1.39	96.02±1.76	95.74±0.98	**96.83±1.00**
	Recall	94.61±0.48	94.07±1.64	95.94±1.39	95.45±2.34	**97.16±1.38**
	F1-Score	94.75±0.79	93.98±0.28	95.98±1.67	95.59±1.94	**96.98±0.97**
Crop Diseases	**Accuracy**	91.34±2.26	92.15±1.13	94.56±2.29	96.12±1.39	**96.35±0.45**
	Precision	91.47±0.47	91.98±2.36	94.63±0.98	95.01±1.22	**96.28±1.82**
	Recall	92.12±0.98	92.05±1.39	95.27±1.55	**96.96±2.43**	96.89±1.56
	F1-Score	91.89±2.52	92.03±1.35	94.90±2.08	95.98±1.28	**96.72±1.95**
CIFAR-10	**Accuracy**	92.56±1.95	93.28±2.59	94.40±0.58	94.12±1.56	**95.74±1.25**
	Precision	92.34±1.36	93.10±2.47	**95.02±0.97**	93.81±2.19	94.56±0.87
	Recall	93.01±1.94	92.72±1.78	94.21±0.91	94.50±0.67	**95.85±1.18**
	F1-Score	92.38±1.39	92.98±0.45	94.39±1.74	94.16±1.08	**95.54±0.99**
Fashion-MNIST	**Accuracy**	91.73±0.57	91.12±1.13	92.67±0.43	92.35±1.36	**93.91±0.98**
	Precision	91.29±1.63	91.35±1.89	92.13±1.39	92.48±1.94	**92.76±1.28**
	Recall	92.18±2.12	90.58±2.56	93.19±0.45	92.72±1.78	**93.84±1.05**
	F1-Score	91.54±0.97	90.94±0.69	92.36±2.06	92.59±1.53	**93.65±0.97**

(including the compound classes) is set to 2 (for the simplicity, other values can also be used). For UCI datasets, we conducted the experiments on the original feature space of samples. For the image datasets, we first extract deep features by the pre-trained ResNet50 model (the deep features before its fully connected layer) [23]. Next, the evidence decision-based pattern classification experiments are conducted on these deep feature spaces. This process for image datasets is shown in Figure 5.

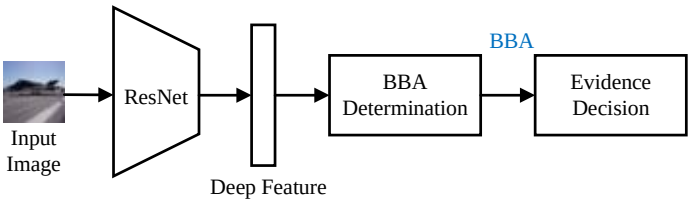

Figure 5. Experiment process for image datasets.

In the experiments, each dataset is divided into two parts, with 50% assigned to the training set and 50% to the test set. The experiment on each dataset is randomly performed ten times. We calculate the average and variance of four measures, including accuracy, precision, recall, and f1-score. The results are shown in Table 3. As we can see, our proposed method performs globally much better than several traditional BBA determination methods on multiple UCI and image datasets (with p-values less than 0.05 in Wilcoxon signed-rank tests), especially for the methods that determine the mass values of compound

focal elements using the singleton focal elements (i.e., the tri-focal element method and the discount-based method). This indicates that by introducing the compound classes and learning mechanism, our E-RBFN offers superior advantages over the traditional heuristic approaches.

5 Conclusions

To better determine the BBA, especially for the mass determination for compound focal elements, we design the BBA determination process as an end-to-end model called E-RBFN. This model can directly determine the mass values of all focal elements (including the singleton and compound ones). Experimental results of evidence fusion decision-based pattern classification on multiple UCI and image datasets show that our method is effective and reasonable.

Note that in our approach, compound-class samples are obtained by the confusion matrix and information entropy, which may depend on the parameter settings. In future work, we will attempt to use the inherent ambiguity or uncertainty in the data to obtain compound-class samples, thus reducing reliance on parameters.

Data Availability Statement

Data will be made available on request.

Funding

This work was supported by National Natural Science Foundation of China under Grant 62473304 and Grant U22A2045.

Conflicts of Interest

The authors declare no conflicts of interest.

Ethical Approval and Consent to Participate

Not applicable.

References

[1] Dempster, A.P. (1967) Upper and Lower Probabilities Induced by a Multivalued Mapping. *The Annals of Mathematical Statistics, 38*, 325-339.

[2] Shafer, G. (1976). *A Mathematical Theory of Evidence*. Princeton University Press.

[3] Richter, S., Bieder, F., Wirges, S., Kinzig, C., & Stiller, C. (2022, July). Sensor data fusion in top-view grid maps using evidential reasoning with advanced conflict resolution. In *2022 25th International Conference on Information Fusion* (*FUSION*) (pp. 1-7). IEEE.[CrossRef]

[4] Sharma, M., & Maity, T. (2022, November). Fault-tolerant multi-sensor data fusion system for underground mine gas hazard prediction using Dempster Shafer Evidence Theory. In *2022 IEEE 6th Conference on Information and Communication Technology* (*CICT*) (pp. 1-5). IEEE.[CrossRef]

[5] Jin, J., Qu, T., Xu, R., Wang, X., & Cichocki, A. (2022). Motor imagery EEG classification based on Riemannian sparse optimization and dempster-shafer fusion of multi-time-frequency patterns. IEEE *Transactions on Neural Systems and Rehabilitation Engineering, 31*, 58-67. [CrossRef]

[6] Zhao, J., Shi, Y., Liu, W., Zhou, T., Li, Z., & Li, X. (2023). A hybrid method fusing frequency recognition with attention detection to enhance an asynchronous brain-computer interface. *IEEE Transactions on Neural Systems and Rehabilitation Engineering, 31*, 2391-2398. [CrossRef]

[7] Sun, L., & Wang, Y. (2018). A multi-attribute fusion approach extending Dempster–Shafer theory for combinatorial-type evidences. *Expert Systems with Applications, 96*, 218-229. [CrossRef]

[8] Xiao, F., Wen, J., & Pedrycz, W. (2022). Generalized divergence-based decision making method with an application to pattern classification. *IEEE transactions on knowledge and data engineering, 35*(7), 6941-6956.[CrossRef]

[9] Han, D., Yang, Y., & Han, C. (2014). Advances in DS evidence theory and related discussions. *Control and Decision, 29*(1), 1-11.

[10] Selzer, F., & Gutfinger, D. (1989, January). LADAR and FLIR based sensor fusion for automatic target classification. In *Sensor fusion: Spatial reasoning and scene interpretation* (Vol. 1003, pp. 236-246). SPIE. [CrossRef]

[11] Bi, Y., Bell, D., & Guan, J. (2004). Combining evidence from classifiers in text categorization. In *Knowledge-Based Intelligent Information and Engineering Systems: 8th International Conference, KES 2004, Wellington, New Zealand, September 20-25, 2004, Proceedings, Part III 8* (pp. 521-528). Springer Berlin Heidelberg.

[12] Zhang, Z., Han, D., & Yang, Y. (2015, October). Image segmentation based on evidential Markov random field model. In *2015 International Conference on Control, Automation and Information Sciences* (*ICCAIS*) (pp. 239-244). IEEE. [CrossRef]

[13] Dezert, J., Liu, Z. G., & Mercier, G. (2011, July). Edge detection in color images based on DSmT. In *14th International Conference on Information Fusion* (pp. 1-8). IEEE.

[14] Jiang, W., Duanmu, D., Fan, X., & Deng, Y. (2012, May). A new method to determine basic probability assignment under fuzzy environment. In

2012 International Conference on Systems and Informatics (ICSAI2012) (pp. 758-762). IEEE.[CrossRef]

[15] Han, D., Han, C., & Deng, Y. (2013). Novel approaches for the transformation of fuzzy membership function into basic probability assignment based on uncertainty optimization. *International Journal of Uncertainty, Fuzziness and Knowledge-Based Systems, 21*(02), 289-322.[CrossRef]

[16] Kang, B. Y., Li, Y. A., Deng, Y., Zhang, Y. J., & Deng, X. Y. (2012). Determination of basic probability assignment based on interval numbers and its application. *Dianzi Xuebao(Acta Electronica Sinica), 40*(6), 1092-1096.

[17] Zhang, S., Han, D., & Yang, Y. (2020). Active learning based on belief functions. *SCIENCE CHINA-INFORMATION SCIENCES, 63*(11).

[18] Smets, P., & Kennes, R. (1994). The transferable belief model. *Artificial intelligence, 66*(2), 191-234. [CrossRef]

[19] Kanungo, T., Mount, D. M., Netanyahu, N. S., Piatko, C. D., Silverman, R., & Wu, A. Y. (2002). An efficient k-means clustering algorithm: Analysis and implementation. *IEEE transactions on pattern analysis and machine intelligence, 24*(7), 881-892. [CrossRef]

[20] Zhu, Q., Cai, Y., & Liu, L. (1999). A global learning algorithm for a RBF network. *Neural Networks, 12*(3), 527-540. [CrossRef]

[21] Asuncion, A., & Newman, D. (2007, November). *UCI machine learning repository*. Retrieved from https://archive.ics.uci.edu/ml

[22] Kaggle. (n.d.). *Kaggle: Your machine learning and data science community*. Retrieved from hhttps://www.kaggle.com

[23] He, K., Zhang, X., Ren, S., & Sun, J. (2016). Deep residual learning for image recognition. In *Proceedings of the IEEE conference on computer vision and pattern recognition* (pp. 770-778).

Wei Li was born in Xianyang, China, in 1997. He received the bachelor's degree in Automation from Huazhong University of Science and Technology, Wuhan, in 2019, and the master's degree in Control Science and Engineering from Xi'an Jiaotong University, Xi'an, in 2022. He is currently pursuing the Ph.D. degree in Control Science and Engineering at Xi'an Jiaotong University. His research interests include evidence theory, information fusion, and pattern classification. (Email: liwei19970705@163.com)

Deqiang Han was born in Xi'an, China, in 1980. He received the bachelor's degree in communication and control engineering and the master's and Ph.D. degrees in control science and engineering from Xi'an Jiaotong University, Xi'an, China, in 2001, 2004, and 2008, respectively. He is currently a Professor with Xi'an Jiaotong University. His research interests include evidence theory, information fusion, and pattern classification. Dr. Han is an International Society of Information Fusion Member and a Technical Program Committee Member for the 1st–12th Chinese Conference on Information Fusion in 2009–2023. (Email: deqhan@xjtu.edu.cn)

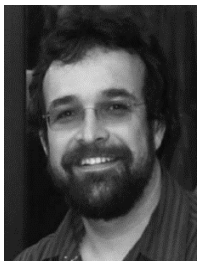

Jean Dezert was born in l'Hay les Roses, France in 1962. He received the electrical engineering degree from the Ecole Franc¸aise de Radio ´ electricit ´ e´ Electronique et Informatique, Paris, France, in ´1985, the D.E.A. degree from University Paris VII (Jussieu), Paris, in 1986, and the Ph.D. degree from University Paris XI, Orsay, France, in 1990, all in automatic control and signal processing. He has been a Senior Research Scientist with the Information and Fusion Systems Research Unit, Information and Modeling and Processing Department, ONERA, Palaiseau, France, since 1993. He gave several invited plenary talks and seminars on information fusion in Europe, America, Australia, and China, during latest years. His current research interests include autonomous navigation, estimation, stochastic systems and their applications to multisensormultitarget tracking, information fusion, and plausible reasoning. Dr. Dezert has served as a Local Arrangements Organizer for the 2000 3rd International Conference on Information Fusion (Fusion) in Paris, and a Secretary, an Executive Vice-President, and the President for the International Society of Information Fusion (ISIF) in 2001, 2004, and 2016, respectively. He has been involved in the Technical Program Committee of Fusion 2001–2016 International Conferences. He was a Board Member of the ISIF. (Email: jean.dezert@onera.fr)

Yi Yang was born in Xi'an, China, in 1980. She received the bachelor's degree in automation from the Xi'an University of Technology, Xi'an, China, in 2002, and the master's and Ph.D. degrees in control science and engineering from Xi'an Jiaotong University, Xi'an, in 2005 and 2010, respectively. She is currently a Lecturer with the School of Aerospace, Xi'an Jiaotong University. Her research interests include evidence theory, pattern classification, and image processing.